

# INTERPLANETARY SCINTILLATION OF RADIO SOURCES AT METRE WAVELENGTHS—II

## THEORY

*A. C. S. Readhead*

(Received 1971 July 23)

### SUMMARY

Interplanetary scintillation is being used, in a survey of radio sources, to study angular structure in the range  $0^{\circ}.1-1''$  at a frequency of 81.5 MHz. The application of diffraction theory to scintillation at this frequency is discussed, and the diffracting parameters of the interplanetary medium are derived. The dependence of scintillation index on angular structure and receiver bandwidth is determined.

### I. INTRODUCTION

A large-scale survey of radio sources at 81.5 MHz is currently in progress. Information about the angular dimensions of the sources can be derived from the variation of scintillation index with solar elongation. The manner in which the observations were carried out and reduced has been described by Hewish & Burnell (1970). The theory has previously been discussed by Little & Hewish (1966) in relation to a survey at 178 MHz (Little & Hewish 1968) but, at 81 MHz, the maximum scintillation occurs at larger elongations than at 178 MHz. The geometry is thus more complicated and some of the assumptions made in the earlier studies are no longer justified. It is not, for example, sufficient to assume that the scattering medium may be represented by a physically thin layer situated where the line of sight is nearest to the Sun. Nor is it sufficient to suppose that all the plasma irregularities give rise to 'far-field' diffraction.

The object of this paper is to develop the more accurate theory required to interpret the 81.5 MHz results. The theory of diffraction by irregular media has recently been extended by Budden & Uscinski (1970) and the application of their work to our problem is discussed in Section 2. In order to use the results it is necessary to adopt a suitable model for the plasma irregularities in the interplanetary medium and in Section 3 an outline is given of recent observations which enable such a model to be determined more precisely than was possible for the earlier survey at 178 MHz. Finally, in Section 4, this model is used to compute scintillation index curves for radio sources of different angular sizes and a simple criterion is derived for finding the angular dimensions of sources from the observational data.

### 2. THEORY

In this section expressions are derived which enable the scintillation index of a radio source to be computed when the line of sight subtends an arbitrary elongation  $\epsilon$  with respect to the centre of the Sun. It is necessary to adopt a model for

the plasma irregularities and the following assumptions, justified in Section 3, are made: (i) the parameters of the medium vary only with radial distance  $r$  from the Sun, and (ii) the autocorrelation function of the electron density variations is gaussian with a width (to  $e^{-1}$ ) given by  $2a(r)$ , and an r.m.s. magnitude given by  $\Delta N_e(r)$ .

Consider the contribution to the total scintillation index  $F$  due to an element  $dz$  of the line of sight as shown in Fig. 1. Under conditions of weak scattering, and for a monochromatic point source, we have (Bramley 1954)

$$dF^2 = \text{constant } \Delta N_e^2(r) a(r) dz = S(r) dz, \quad (1)$$

where  $S(r)$  defines the *scattering power* of the medium at distance  $r$  from the Sun. This expression is only valid for the far-field, i.e. for a sufficiently large value of  $z$ .

In practice  $dF^2$  may be smaller than the value given by equation (1) on account of the finite angular size of the source, the decorrelation of scintillation across the finite receiver bandwidth, and the effect of the Fresnel cut-off in the near field. An expression for the reduction factor  $A$  due to these effects, which is valid under conditions of weak scattering, has been derived by Budden & Uscinski (1970).

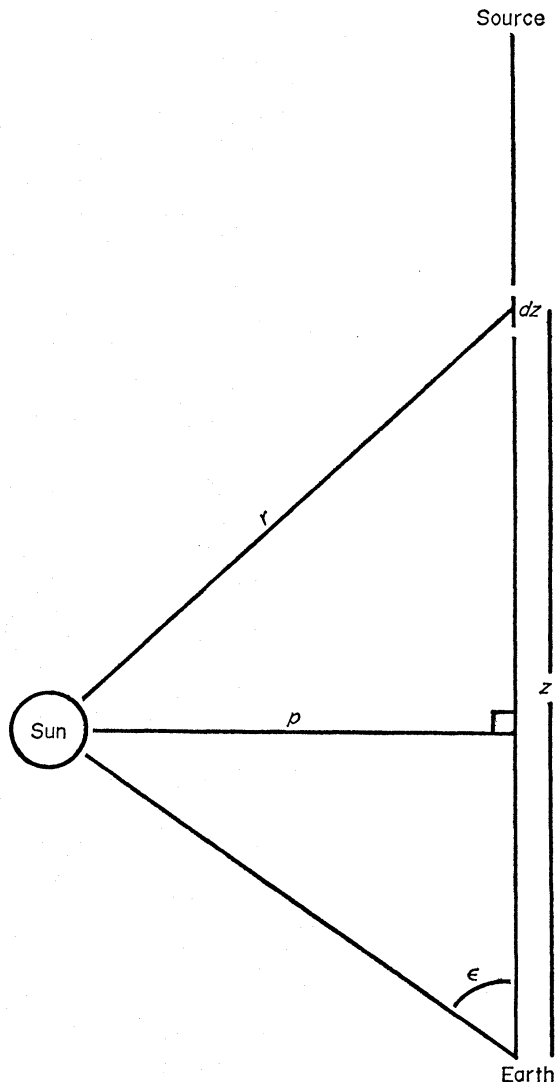


FIG. 1. *The geometry of the diffracting medium.*

In the case of a source with a gaussian brightness distribution observed with a receiver having a resonance bandpass function,  $A$  is given by their equation (8o):

$$A(f, b, h) = f^2 / (1 + h^2 + fb) [(1 + h^2 + fb)^2 + f^2]$$

where  $h^2 = 2(z\theta_0/a)^2$

$$f = 4z/a^2k$$

$2b$  = half-power bandwidth/frequency

$k$  = the wavenumber

$2\theta_0$  =  $1/e$  width of the gaussian brightness distribution

$z$  = the distance of the screen from the observer.

Thus we have  $dF^2 = S(r)A(f, b, h) dz$ . Now provided  $dz \gg a$ , so that adjacent elements  $dz$  contain uncorrelated irregularities, this expression may be integrated, giving

$$F^2(\epsilon) = \int_{\text{diffracting medium}} S(r)A(f, b, h) dz. \quad (2)$$

The theory leading to (2) is only valid provided the scattering is weak. As we shall see in Section 3 this is so at large elongations. We therefore make use of (2) only at elongations greater than  $35^\circ$ , for which the errors are less than 5 per cent. Unfortunately no relation analogous to (2) has yet been derived for an extended medium under the conditions of multiple scatter which apply for  $\epsilon < 35^\circ$ . An approximate result may, however, be obtained (Little & Hewish 1966) by assuming that the scattering is localized in a physically thin region at the point of closest approach of the line of sight to the Sun. It should be stressed immediately that no attempt will be made to use data for  $\epsilon < 35^\circ$  in the derivation of source diameters although, as will be seen, such data are of value in estimating the parameters of the plasma irregularities.

For the 'thin-screen' case the reduction of scintillation index depends only upon the angular spread of the scattered radiation, irrespective of whether weak or strong scattering is involved (Little & Hewish 1966; Little 1968). Application of Mercier's (1962) results for the angular spectrum of multiple scattering then shows that the same expression for  $A$  still holds, provided that  $a(r)$  is replaced by  $a(r)/\sqrt{2}\phi(r)$ , where  $\phi(r)$  is the total r.m.s. phase deviation in radians introduced along the line of sight. This expression for  $a(r)$  is used when  $\phi(r) > 1$ , i.e. in the present case for elongations less than  $17^\circ$ . Since, in addition,  $F = 1$  for an ideal monochromatic point source under conditions of multiple scattering we have the simple result

$$F^2(\epsilon) = A(f, b, h) \text{ for } \epsilon < 17^\circ \text{ at } 81.5 \text{ MHz.} \quad (3)$$

For the intermediate region  $17^\circ < \epsilon < 35^\circ$  no adequate theory exists and it is only possible to make estimates of  $F(\epsilon)$  by interpolation between the regions discussed above.

### 3. THE INTERPLANETARY MEDIUM

In order to make numerical computations using the expressions derived in the previous section the scattering power  $S(r)$  and the scale  $a(r)$  of the plasma irregularities must be specified. Both of these functions may be obtained from scintillation observations.

### The scattering power $S(r)$

In Fig. 2 we show observations of  $F$  plotted as a function of  $p = \sin(\epsilon)$  for a number of sources observed at different frequencies. Since, for an ideal point source and weak scattering we have  $F \propto \nu^{-1}$ , where  $\nu$  is the frequency it is convenient to plot  $F\nu$  as ordinate, rather than  $F$ , in order to make an appropriate scaling. The observations in Fig. 2 were made by Little & Hewish (1968), Bourgois (1969), Cohen & Gundermann (1969) and Burnell (Ph.D. Thesis). Results obtained by long base-line interferometry indicate that the sources chosen approximate to ideal point sources.

It is clear that the observations in Fig. 2, which include frequencies between 2.6 GHz and 81.5 MHz, can be represented by a single line of constant slope provided that the frequency dependent 'turn-overs' (resulting from the departure

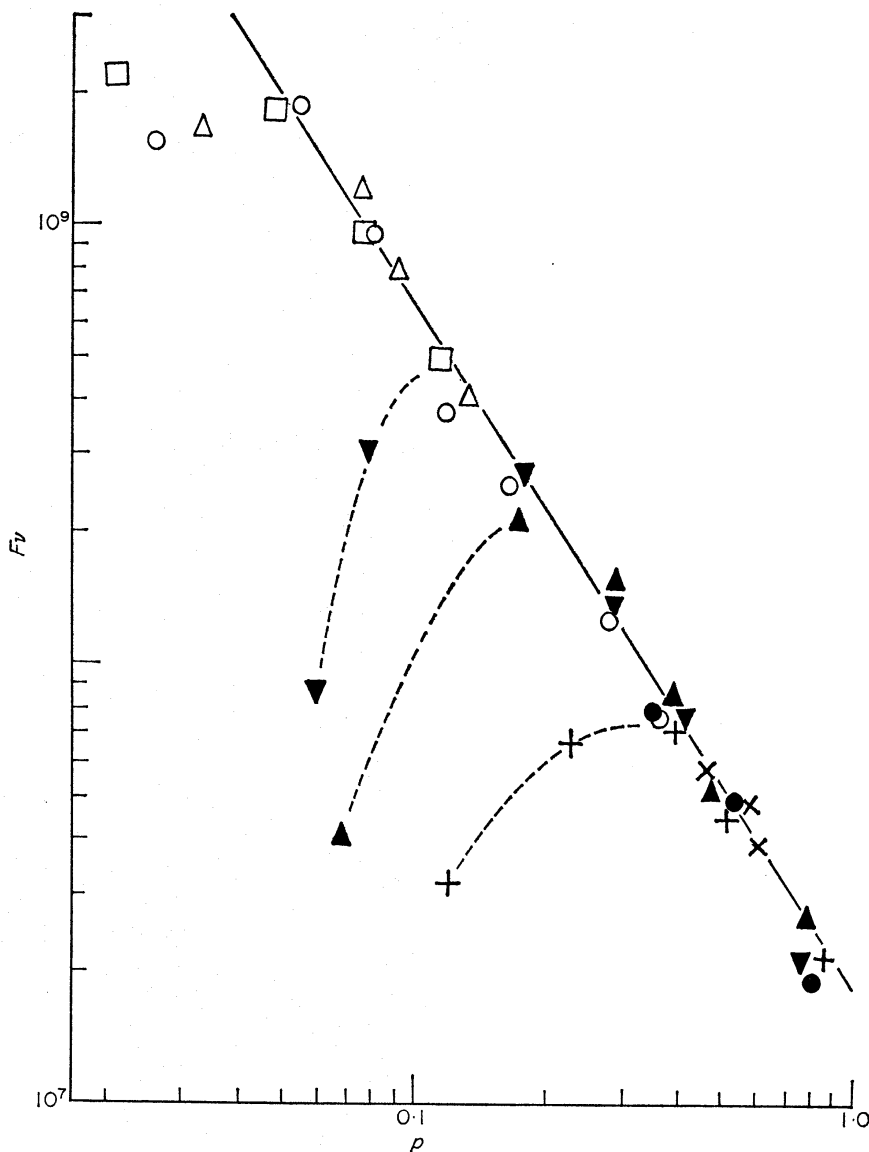


FIG. 2. The variation of scintillation index with  $p$ . Observations by Bourgois:  $\square$  P1148-00,  $\triangle$  CTA 21,  $\circ$  3C 279 (2695 MHz); Cohen *et al.*:  $\nabla$  CTA 21 (610 MHz),  $\blacktriangle$  CTA 21 (428 MHz),  $\bullet$  3C 279 (195 MHz); Little and Hewish:  $+$  3C 138 (178 MHz); and Burnell:  $\times$  (81.5 MHz).

of  $A$  from unity) are ignored. The simplest model which can reproduce this result is a power law variation of scattering with radial distance from the Sun. Thus we have assumed that  $S(r)$  approximates to a simple power law  $S(r) = Br^{-\alpha}$  where  $B$  is a constant.

An estimate of the value of  $\alpha$  may be obtained from the relation

$$F^2(p) \sim \int_{-\infty}^{\infty} S(r) dz = \int_{-\infty}^{\infty} Br^{-\alpha} dz \quad (4)$$

where the limits of integration ignore the fact that the Earth is embedded in the medium. The data in Fig. 2 yield

$$F(p) = 0.22p^{-1.55 \pm 0.05} \text{ at } 81.5 \text{ MHz}$$

and the analytical solution of the integral equation gives

$$S(r) = 3.24 \times 10^{-2} r^{-4.1 \pm 0.1} \text{ A.U.}^{-1}, \text{ where } r \text{ is in A.U.}$$

A more accurate result, using numerical integration over the line of sight from the Earth to infinity, gives

$$S(r) = 3.77 \times 10^{-2} r^{-4.0} \text{ A.U.}^{-1} \quad (5)$$

and this is the expression which will be used hereafter.

### The scale $a(r)$

It is well known that, for weak scattering in the far field, the autocorrelation function of the diffraction pattern is the same as that of the electron density variations in the medium (Ratcliffe 1956). Measurements of the autocorrelation function of the diffraction pattern have been made by Dennison & Hewish (1967), and Hewish & Symonds (1969) and Symonds (Ph.D. Thesis), while other estimates from the temporal power spectra of scintillations observed at a single site have been obtained by Cohen & Gundermann (1969).

These results have been discussed by Jokipii & Hollweg (1970) who suggest that the irregularities have a wavenumber power spectrum which follows a power law between upper and lower limits and in consequence, the autocorrelation function of the diffraction pattern is not simply related to the scale-size of the irregularities. Hewish (1971) and Little (1971), however, have shown that scintillation data taken at widely different frequencies are in conflict with Jokipii and Hollweg's model. Large-scale irregularities revealed by space-probes may, indeed, have a power-law spectrum, but the same spectrum cannot extend to the scale-sizes responsible for scintillation. For the latter a gaussian autocorrelation function appears to give the best description. In Fig. 3 results obtained assuming a gaussian autocorrelation function are shown. These results are derived from measurements of the angular spectrum by Okoye & Hewish (1967), and from spaced receiver measurements by Symonds (Ph.D. Thesis). On the basis of these observations we assume a power law variation for the scale size given by

$$a(r) = a_0 r^\beta. \quad (6)$$

Since  $a(r)$  varies along the line of sight the autocorrelation function of the diffraction pattern corresponds to a weighted average of  $a(r)$ . In order to determine  $a(r)$  from the observations consider an element  $dz$  of the line of sight. This produces

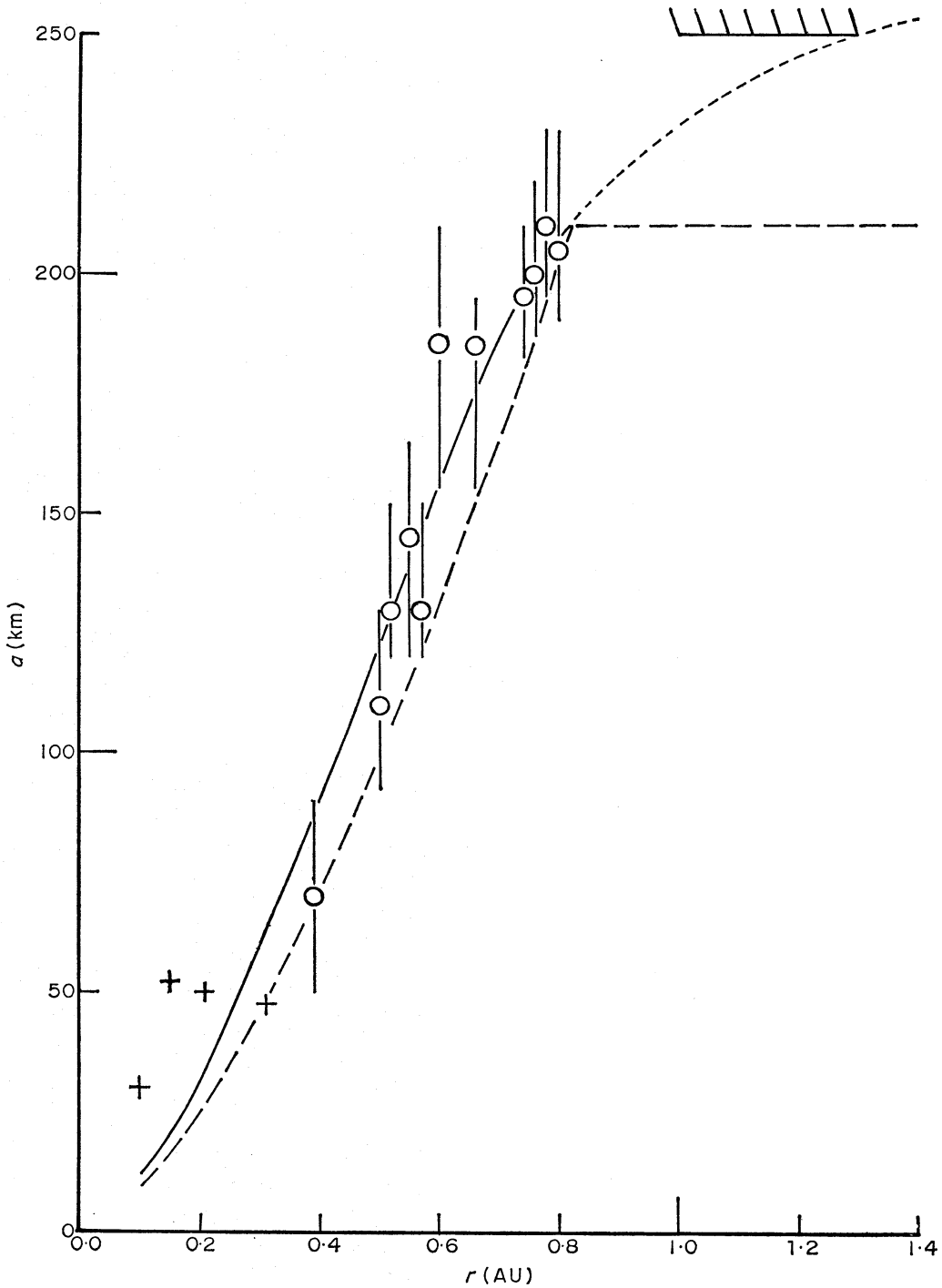


FIG. 3. The scale size of the irregularities in the interplanetary medium. Observations are by Okoye and Hewish (+), and by Symonds (O). Curves show the assumed scale — — —, and the corresponding observed scale ———. Also shown are the upper limit to the scale in the region between 1.0 and 1.3 A.U. and the possible variation of the scale in this region ———.

a diffraction pattern which has an autocorrelation function  $\rho_x$  given by

$$\rho_x = S(r) \exp \left[ -x^2 / (a(r))^2 \right] dz \quad (7)$$

where  $x$  is a length coordinate in a plane perpendicular to  $z$ .

Integrating along a line of sight, and assuming as before that  $dz \gg a(r)$  so that the diffraction patterns due to different elements  $dz$  are uncorrelated, we obtain a resultant autocorrelation function

$$\rho_x(\epsilon) = \int_{\text{medium}} S(r) \exp[-x^2/(a(r))^2] dz. \quad (8)$$

The forms of  $\rho_x(\epsilon)$  calculated from (8) for  $\beta = 1, 2, 3$  and using the previously determined expression for  $S(r)$  are shown in Fig. 4. The curves are still roughly gaussian and fall to  $e^{-1}$  in a distance

$$\rho_x = a_0(r) (1 + 0.14\beta)$$

and the observations of Fig. 3 suggest that a reasonable approximation to the radial variation, for  $r < 0.8$ , is obtained by putting  $\beta = 1.5$  so that

$$a(r) = 1.88 \times 10^{-6} r^{1.5} \text{ A.U.} \quad (\text{For } r < 0.8 \text{ A.U.}). \quad (9)$$

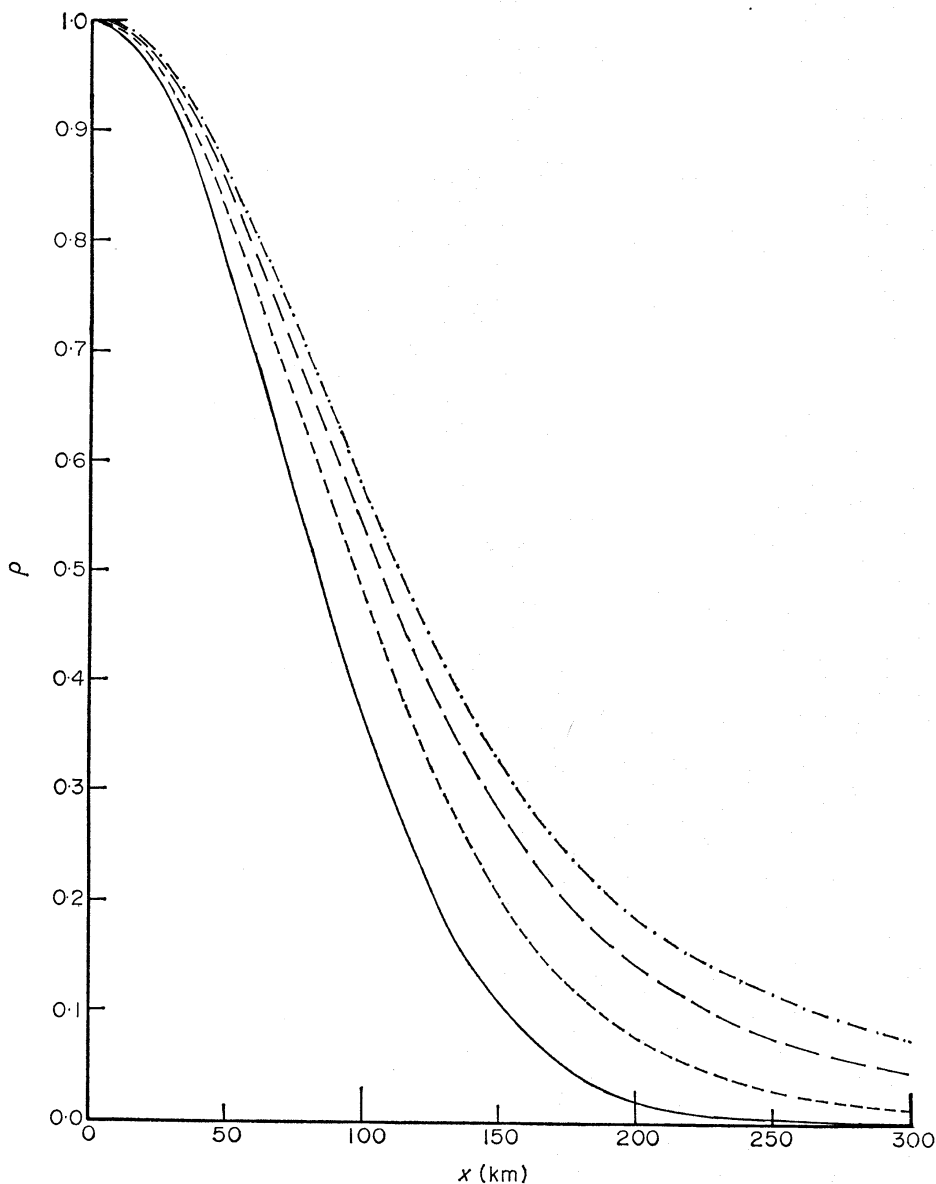


FIG. 4. The autocorrelation function of the irregularities. The curves show the autocorrelation function at  $r = 0.5$  A.U. —; and the corresponding observed autocorrelation functions for various values of  $\beta$ : - - -  $\beta = 1$ , - - -  $\beta = 2$ , - · - ·  $\beta = 3$ .

There is an indication that  $\beta$  may decrease for radial distances exceeding about 0.8 A.U.

Since  $a(r)$  is known with less accuracy than  $S(r)$  it is desirable to check equation (9) by seeing whether computed  $F(\epsilon)$  curves correspond with observed  $F(\epsilon)$  curves. If there were a source of known angular size in the range  $0''.1-0''.5$  a direct comparison of observation and theory could be made. Unfortunately scintillation techniques currently afford the only means of angular diameter measurement in this range at 81.5 MHz so that no independent calibration is possible and only the internal consistency can be checked.

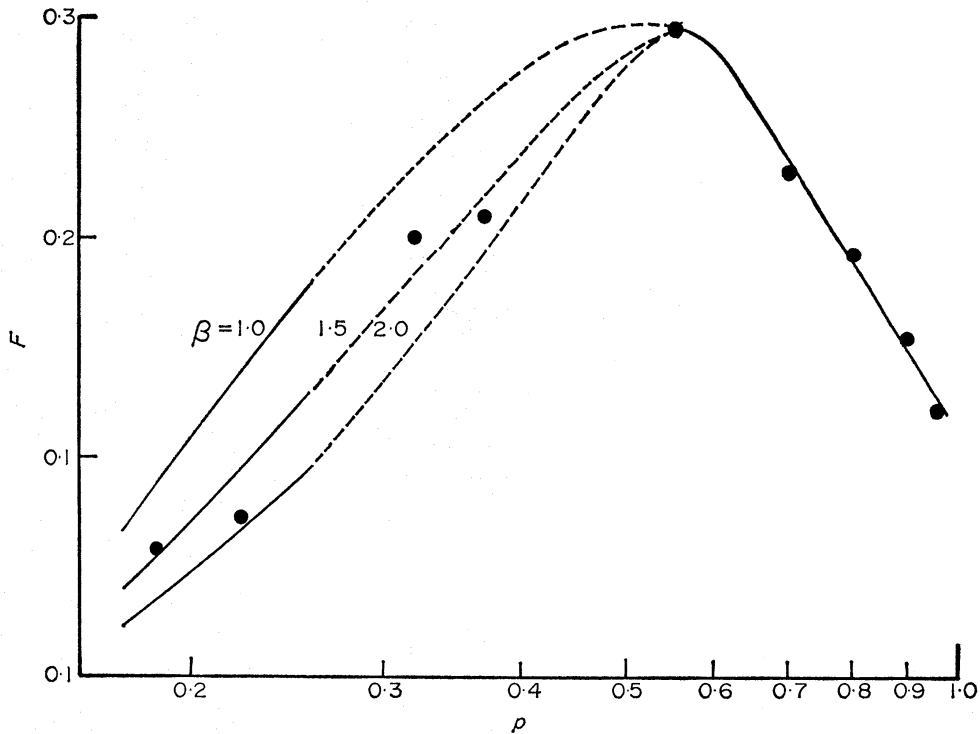


FIG. 5. The scintillation index at small elongations. The theoretically predicted variation of  $F$  for different values of  $\beta$  is shown. Observations of 3C 241 by the author ( $\bullet$ ).

An observed  $F(\epsilon)$  curve obtained as described by Hewish & Burnell (1970) is shown in Fig. 5. The features of this curve may be used to check our model. The rapid decrease of  $F$  for  $\epsilon < 20^\circ$  is governed both by the radial index  $\beta$  and by the integrated phase deviation along a line of sight; the latter depends upon  $S(r)$  and is well determined. By comparing observed and theoretical  $F(\epsilon)$  curves for  $\epsilon < 20^\circ$  it is possible to check  $\beta$ .

A series of theoretical curves, computed from (3) and (9) by the method described in Section 4, is shown in Fig. 5. It may be seen that the adopted value  $\beta = 1.5$  gives a good fit in the region  $\epsilon < 20^\circ$ , whereas putting  $\beta = 1$  gives too slow and  $\beta = 2$  too rapid a decrease below  $20^\circ$ . This analysis therefore confirms our value of  $\beta = 1.5$  derived from independent observational evidence.

Now that both  $S(r)$  and  $a(r)$  have been determined it is possible to use (2) to calculate  $F(\epsilon)$ . The contribution to the scintillation index, of a monochromatic point source, from different parts of the interplanetary medium along the line of sight is shown in Fig. 6.

By using the values for  $S(r)$  and  $a(r)$  given in (5) and (9) in expression (2) we may now compute  $F(\epsilon)$ , for a source of given angular size  $2\theta_0$ , in the range



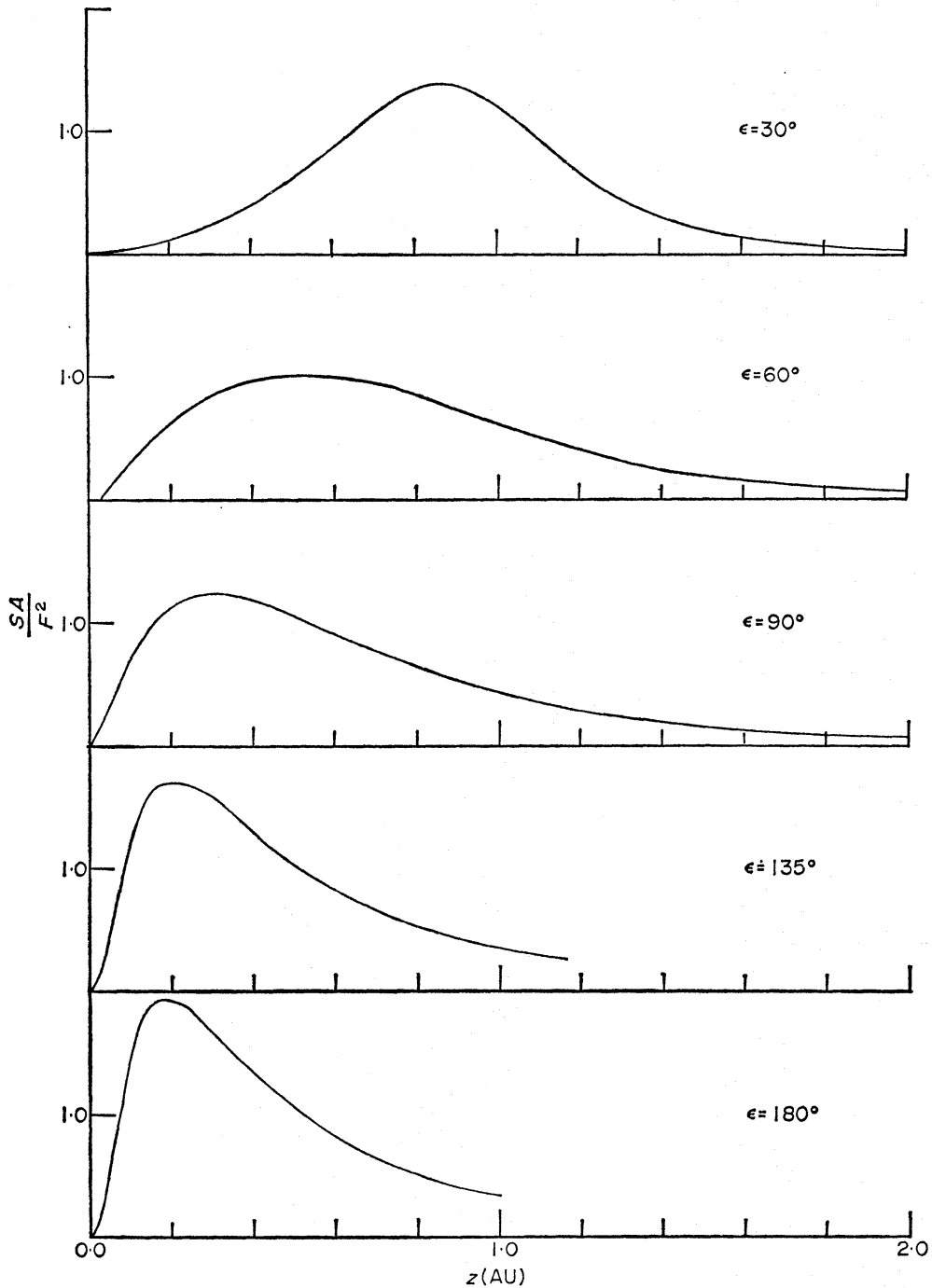


FIG. 6. *The contribution to  $F^2$  from different parts of the interplanetary medium.*

$35^\circ < \epsilon < 90^\circ$ . This is done in Section 4 where a series of  $F(\epsilon)$  curves are derived by this method. Comparison of these curves with the observed scintillation index curve in the range  $35^\circ < \epsilon < 90^\circ$  gives an estimate of the angular diameter of the source.

#### *The medium in the range $r > 1 \text{ A.U.}$*

Observations of  $F(\epsilon)$  for  $\epsilon > 90^\circ$  give information about the medium for  $r > 1 \text{ A.U.}$  Since there are large uncertainties in both  $S(r)$  and  $a(r)$  in this region

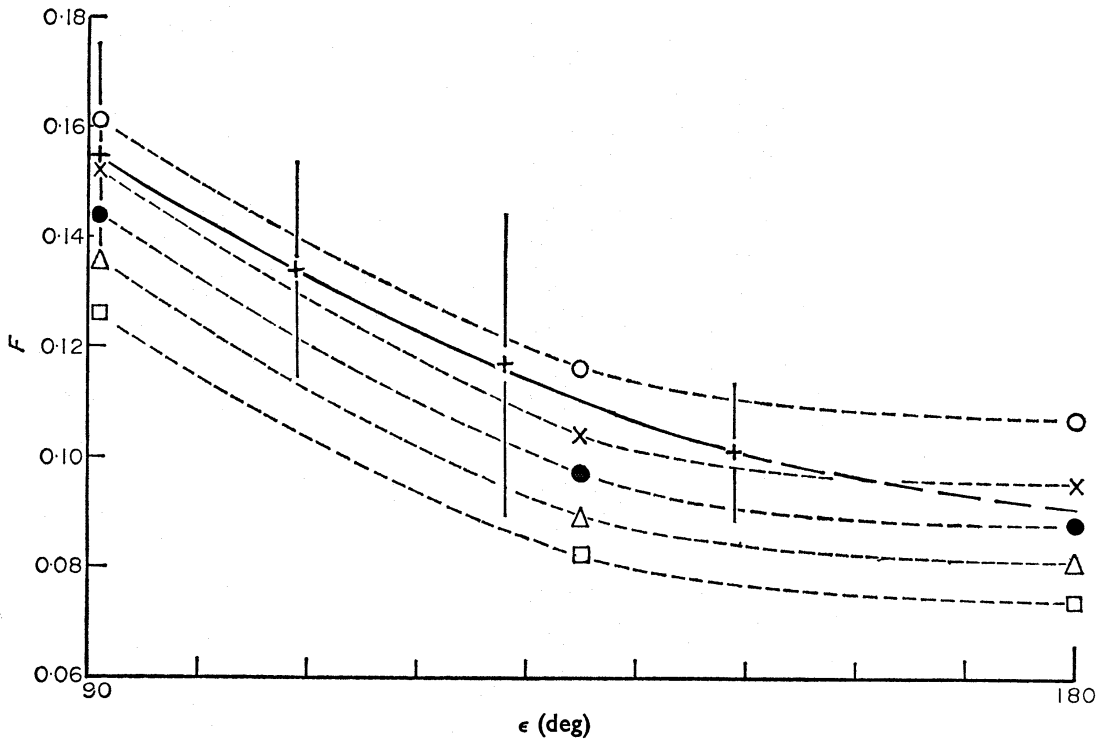


FIG. 7. The scintillation index at large elongations. Observations by Burnell (+), theoretical predictions (i) assuming no near-field correction (O); and (ii) including the near-field correction for scales: 150 km (x), 200 km (●), 250 km (Δ), and 300 km (□).

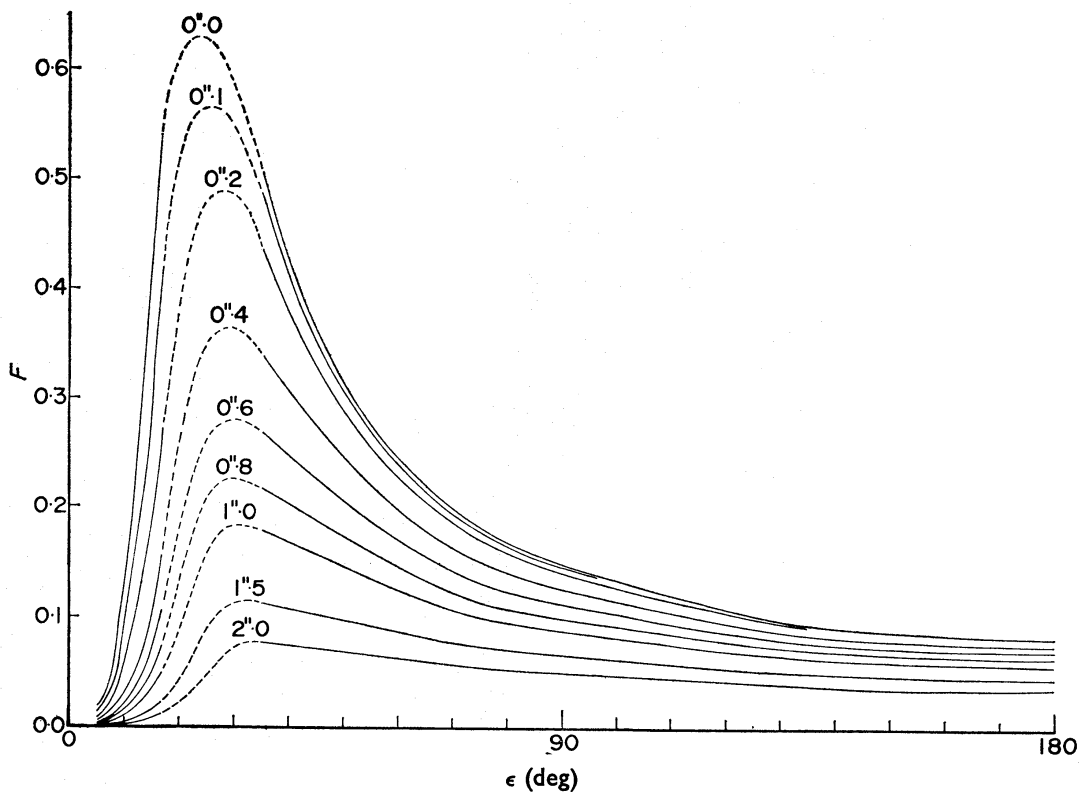


FIG. 8. Scintillation index curves for sources of different angular size,  $2\theta_0$ , observed with a receiver having a bandwidth of 1 MHz. The dashed portions are interpolations between elongations  $17^\circ$  and  $35^\circ$ .

we include this discussion here only to obtain rough estimates of the behaviour of  $F$  and the results are not used in the derivation of source sizes.

Fig. 7 shows a comparison between observed and theoretically predicted values of  $F$ . The data are averages over  $20^\circ$  intervals of observations, of a number of small sources, made by Burnell (Ph.D. Thesis). We have assumed that  $S(r)$  preserves the form given in (5) out to 2 A.U. This assumption seems to be reasonable (at least out to about 1.3 A.U.) since the observations lie close to the theoretical curve without near-field effects being taken into account. Also shown are the theoretical

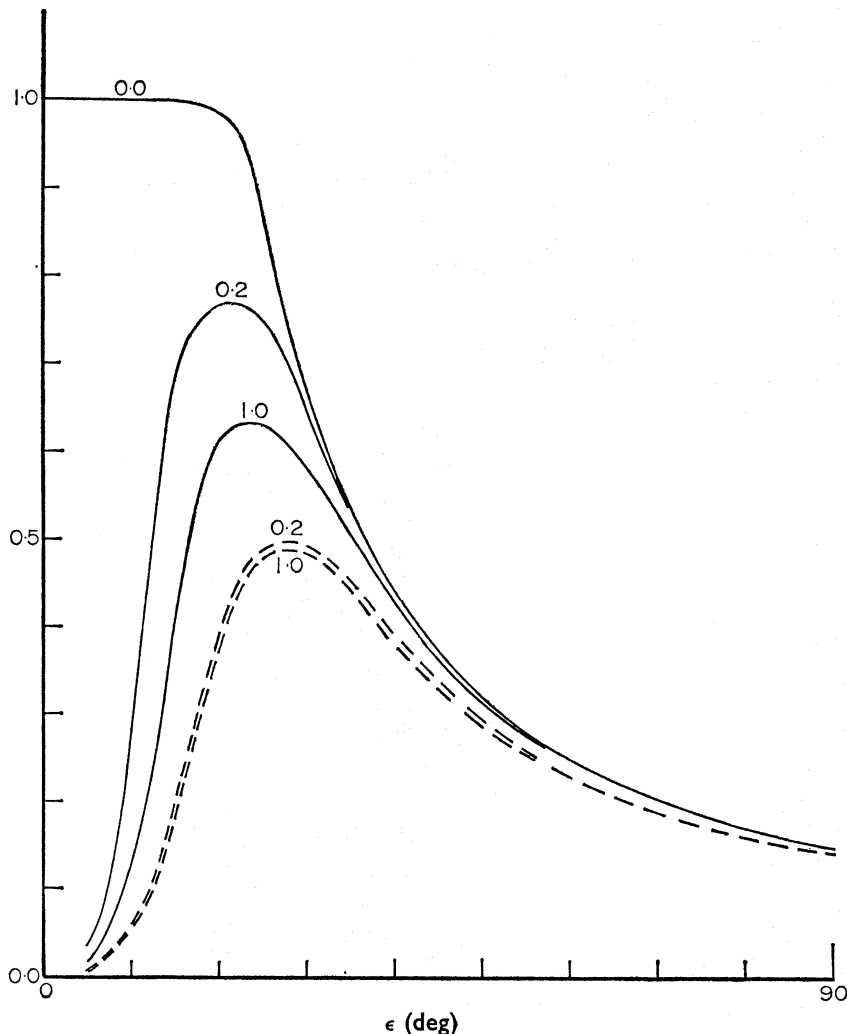


FIG. 9. The dependence of scintillation index on receiver bandwidth and source size. The curves correspond to a point source ———, observed with a monochromatic receiver, and with receivers having bandwidths of 0.2 MHz, and 1.0 MHz; and a 0".2 source - - -, observed with receivers having bandwidths of 0.2 MHz, and 1.0 MHz.

curves including the near-field effect (given by  $A$ ), for a number of scale sizes assumed independent of radial distance. We see that putting  $a > 250$  km gives curves which fall consistently below the observed values, so that this value may be taken as an upper limit. Fig. 6 shows that the main contribution to scintillation index comes from the region  $r < 1.3$  for  $\epsilon > 90^\circ$ . Thus the upper limit derived here for the scale size applies strictly only to this region. In deriving scintillation index

curves we assume a scale size of the form given by (9) for  $r < 0.82$  A.U. and a scale independent of  $r$  given by

$$a = 1.4 \times 10^{-6} \text{ A.U. for } r > 0.82 \text{ A.U.} \quad (10)$$

This scale size variation, together with the resulting observed scale size, is plotted in Fig. 3.

Finally, some justification should be given for the assumption concerning spherical symmetry of the scattering medium about the Sun. In the earlier model used by Little & Hewish (1966) a small variation with heliocentric latitude was assumed. This was based on direct measurements of angular scattering which exhibited such a variation for  $\epsilon < 30^\circ$ . In the present instance we are mainly concerned with the region  $\epsilon > 35^\circ$  for which the observations of  $F(\epsilon)$  show no significant heliocentric latitude dependence. A similar conclusion has been reached by Cohen, Gundermann & Harris (1967).

#### 4. COMPUTED $F(\epsilon)$ CURVES

Relations (2) and (3) were employed to compute  $F(\epsilon)$  curves for gaussian sources of varying angular diameter using the model defined by relations (5), (9) and (10). In the computation the medium was divided into spherical shells of

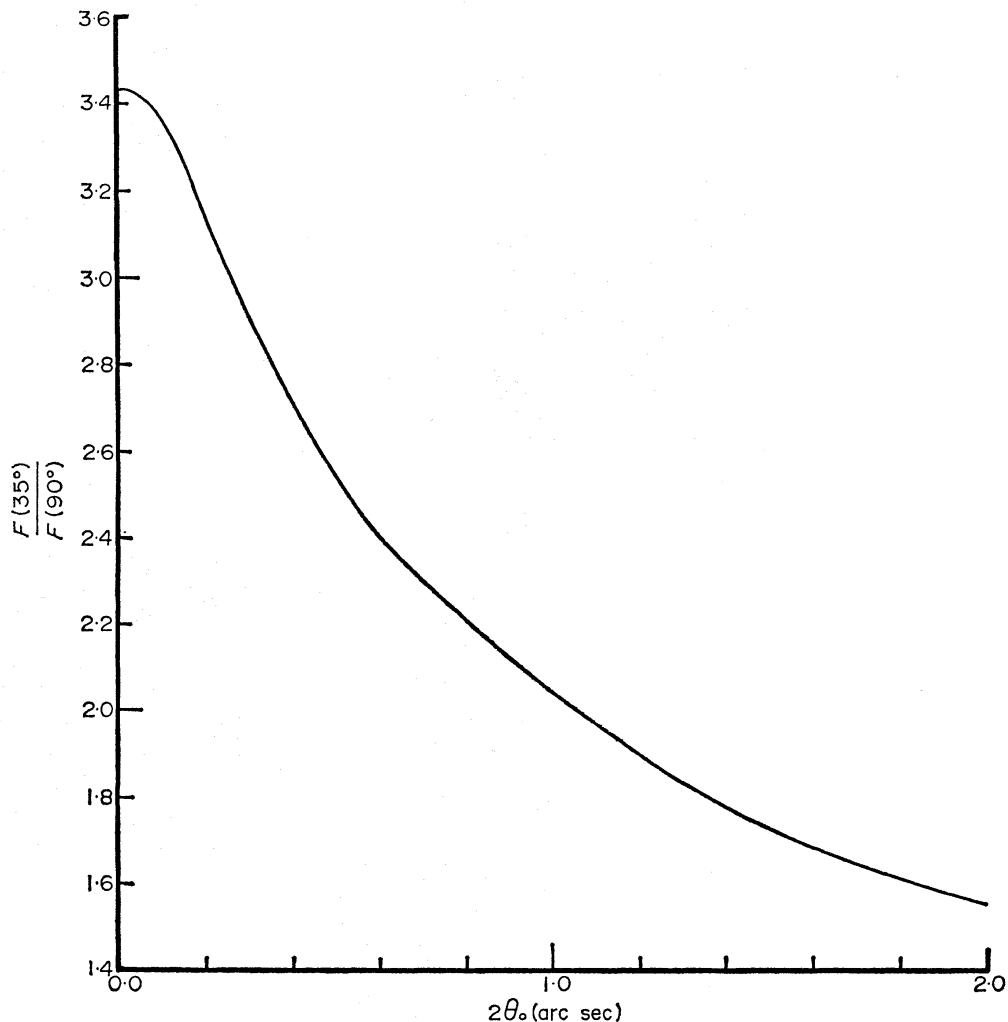


FIG. 10. The variation of  $F(35^\circ)/F(90^\circ)$  with source size.

thickness  $\sim 0.005$  A.U. and the integration was performed over a range of  $z$  extending from the Earth to  $z = 2$  A.U. Rounding-off errors due both to the shell approximation, and to the termination of the integration, amounted to less than 5 per cent. The computed curves are shown in Fig. 8, where the broken lines denote interpolation between  $\epsilon < 17^\circ$  and  $\epsilon > 35^\circ$  as discussed in Section 3.

In the survey at 81.5 MHz a bandwidth of 1 MHz is used and the effect of the departure from monochromaticity is shown by the curves in Fig. 9. From this figure we see that decorrelation of scintillation across the bandwidth is important only for sources of size  $< 0''.2$  when observed at  $\epsilon < 20^\circ$ .

It is immediately apparent from Fig. 8 that the maxima of the scintillation index curves occur at roughly the same value of  $\epsilon$  regardless of the angular diameter of the source. In order to estimate the source dimensions from observed  $F(\epsilon)$  curves it is therefore necessary to use the slope of the  $F(\epsilon)$  curve in the region  $\epsilon > 35^\circ$ . The value of the ratio  $F(35^\circ)/F(90^\circ)$ , for sources of different angular diameter, is plotted in Fig. 10.

This figure indicates that it should be possible to measure angular diameters in the range  $0''.1-1''.5$  with reasonable accuracy. The accuracy decreases rapidly above  $2''.0$  and in practice it is unlikely that the method can be applied to angular diameters exceeding  $1''.5$ , except for the most intense sources.

#### ACKNOWLEDGMENTS

I thank Dr A. Hewish for his help and encouragement, and for many useful discussions. I also thank my father, C. T. Readhead, for financial support during the early part of this work, and I gratefully acknowledge the support of an Isaac Newton Studentship received during the course of this work.

*Mullard Radio Astronomy Observatory, Cavendish Laboratory, Cambridge*

#### REFERENCES

- Bourgois, G., 1969. *Astr. Astrophys.*, **2**, 209.  
 Bramley, E. N., 1954. *Proc. R. Soc.*, **A225**, 515.  
 Budden, K. G. & Uscinski, B. J., 1970. *Proc. R. Soc.*, **A316**, 315.  
 Cohen, M. H., Gundermann, E. J. & Harris, D. E., 1967. *Astrophys. J.*, **150**, 767.  
 Cohen, M. H. & Gundermann, E. J., 1969. *Astrophys. J.*, **155**, 645.  
 Dennison, P. A. & Hewish, A., 1967. *Nature, Lond.*, **213**, 343.  
 Hewish, A. & Symonds, M. D., 1969. *Planet. Space Sci.*, **17**, 313.  
 Hewish, A. & Burnell, S. J., 1970. *Mon. Not. R. astr. Soc.*, **150**, 141.  
 Hewish, A., 1971. *Astrophys. J.*, **163**, 645.  
 Jokipii, J. R. & Hollweg, J. V., 1970. *Astrophys. J.*, **160**, 745.  
 Little, L. T. & Hewish, A., 1966. *Mon. Not. R. astr. Soc.*, **134**, 221.  
 Little, L. T. & Hewish, A., 1968. *Mon. Not. R. astr. Soc.*, **138**, 393.  
 Little, L. T., 1968. *Planet. Space Sci.*, **16**, 749.  
 Little, L. T., 1971. *Astr. Astrophys.*, **10**, 301.  
 Mercier, R. P., 1962. *Proc. Camb. phil. Soc. math. phys. Sci.*, **58**, 382.  
 Okoye, S. E. & Hewish, A., 1967. *Mon. Not. R. astr. Soc.*, **137**, 287.  
 Ratcliffe, J. A., 1956. *Rep. prog. Phys.*, **19**, 188.